

Star Tracking through the Exhaust Beam of Mercury Bombardment Thrusters

NELSON L. MILDER* AND JAMES S. SOVEY†
NASA Lewis Research Center, Cleveland, Ohio

A 0.5-m focal length, plane grating monochromator is used to measure the radiance of spectral radiation emanating from regions downstream of a mercury bombardment thruster. The wavelength range investigated is 2800–6000 Å. This radiation is due primarily to the radiative decay of excited mercury atoms exhausted from the thruster. Radiance values ranged from 10^{-11} to 10^{-9} w/cm² sterad, varying with wavelength. For resonant radiation, the spectral radiance exceeds 10^{-8} w/cm² sterad. From such radiance measurements, it is concluded that the thruster background radiation should not interfere with the control functions of a star tracker viewing through the thruster exhaust, provided that the tracker is designed to operate with a sufficiently small field of view. Problems may be encountered, however, during the spacecraft acquisition phase where a larger field of view may be required. Here the thruster exhaust radiation may be comparable to the star light flux. This problem may be circumvented by locating the tracker view axis so as not to view downstream of the thruster.

Nomenclature

A	= entrance aperture area, cm ²
$F(\lambda)$	= phototube radiant sensitivity, amp/w
$f(\lambda)$	= fraction of phototube signal due to reflected light
I_λ	= radiant flux of standard lamp, w/cm ²
i_s	= star flux current, amp
L	= superscript denoting lamp
$M(\lambda)$	= star spectral power density, w/(cm ²)(μ)
$N(\lambda)$	= thruster background radiances, w/(cm ²)(sterad)
$Q(\lambda)$	= spectral radiance of lamp, w/(cm ²)(sterad)(μ)
$R(\lambda)$	= transmissivity of the optical system
$S(\lambda)$	= phototube signal, amp
$\Delta\lambda$	= bandwidth, μ
θ	= angular field of view, radian
λ	= wavelength, Å
Ω	= solid angle subtended by monochromator exit slit, sterad

Subscripts

ch	= thruster chamber
T	= thruster
v	= volume

Introduction

ELECTRIC propulsion systems consisting of ion thrusters are presently being considered for use on proposed spacecraft such as the Applications Technology Satellite (ATS), Pioneer G and H, and the Communication Technology Satellite (CTS, to be launched in a joint program between Canada and the U.S.). These spacecraft may use optical systems either for guidance and attitude control (star trackers) or as part of the science package to measure uv and ir radiation. Depending on the location of such systems with respect to the ion thrusters, radiation emanating from thruster exhaust plumes could interfere with the operation of these optical devices. Recently, it has been suggested that photo-excitation by sunlight of expelled un-ionized propellant from cesium ion thrusters may introduce radiation into the tracking system.¹

In an earlier work² as well as in the present work, it is proposed that a more serious problem than photoexcitation by sunlight may be thruster produced spontaneous emission of

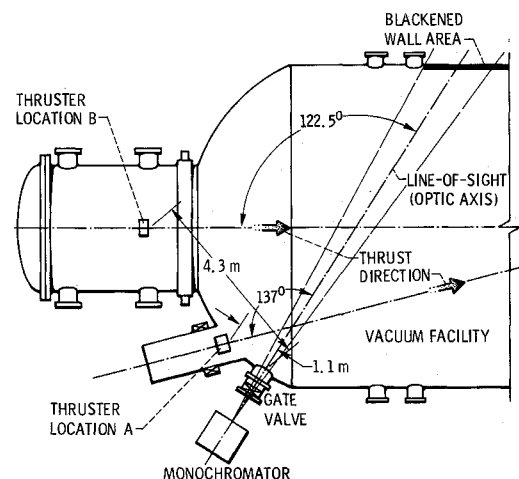


Fig. 1 Experimental arrangement.

excited atoms in regions downstream of a mercury bombardment thruster. In the present study, spectral radiances were obtained at a fixed detector (monochromator) position relative to two thruster locations as shown in Fig. 1. The wavelength range investigated was from approximately 2800–6000 Å. The thrusters used in this investigation represent the latest state-of-the-art design.³

Experiment

Experimental Arrangement

Two 30-cm diam, hollow cathode mercury bombardment thrusters were arranged in a 7.6-m-diam by 18.3-m-long vacuum tank as shown in Fig. 1. The thrusters were located at different positions relative to the optical detecting system. These positions are labeled A and B to facilitate discussion. The distance between the thruster at location A and the viewing port of the optical system was 1.1 m. For the thruster at location B this distance was 4.3 m. For thruster location A the optical line of sight and the thruster axis were coplanar; whereas for thruster location B, the plane of the thruster axis was about 0.3 m above the plane of the optical line of sight. The angles formed by the optic axis and the thruster axes are 137° for thruster position A and 122.5° for thruster position B. The thrusters incorporated the most recent design concepts,³ including high perveance "dished grid" optics. A plasma bridge neutralizer⁴ was used to provide electrons for ion beam neutralization. The net ion beam extraction voltage was

Presented as Paper 72-441 at the AIAA 9th Electric Propulsion Conference, Bethesda, Md., April 17–19, 1972; submitted April 27, 1972; revision received August 28, 1972.

Index categories: Spacecraft Propulsion Systems Integration; Spacecraft Navigation, Guidance, and Flight-Path Control Systems; Electric and Advanced Space Propulsion.

*Physicist, Electric Propulsion Branch. Member AIAA.

†Aerospace Research Engineer, Electric Propulsion Branch.

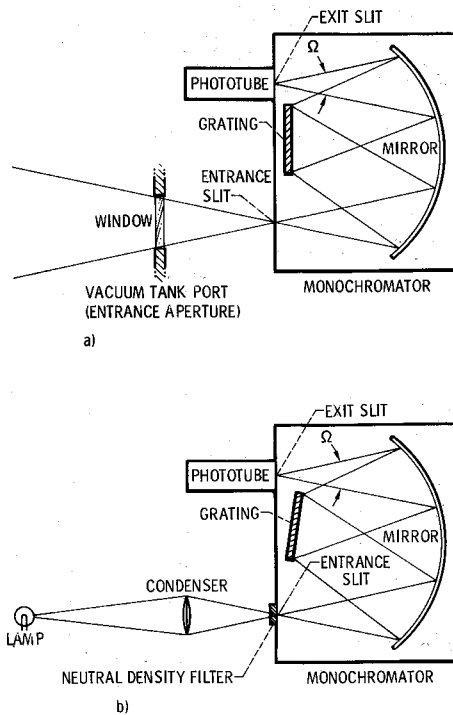


Fig. 2 Optical arrangements. a) Optics for thruster beam radiances. b) Optics for calibration data.

800–1000 v, and the accelerator voltage was –400 to –500 v for both thrusters. Thruster beam currents were 1.5 amp and propellant utilization generally exceeded 85% in all tests. The thrusters were operated separately for each test in which spectral data were obtained. During thruster operation the vacuum tank pressure was maintained at approximately 10^{-7} torr, rising about a decade in the vicinity of the thruster.

Optical System

A 0.5-m, focal-length Ebert mount, plane grating monochromator with matched entrance and exit slits was used to measure spectral radiances resulting from radiation emanating from regions downstream of the thrusters. A schematic drawing of the optical system is shown in Fig. 2a. The effective entrance aperture consisted of a 2.5-cm-thick by 15.2-cm-diam quartz window mounted at a 30-cm-diam vacuum tank port. The port was equipped with a gate valve to facilitate cleaning of the port window as well as to protect the window against sputter coating from thruster and facility components when the port was not in use.

In Fig. 2a the relationship between the viewing port window (entrance aperture) and the monochromator is shown. The thruster light in the vacuum chamber represented an extended source, so that the principal rays shown in the figure defined the solid angle subtended by the source and the monochromator entrance slit. Projecting these rays through the monochromator optics demonstrated that the grating was completely filled with light. Thus no condensing lens external to the monochromator could provide an improvement in illumination at the exit slit of the monochromator.⁵ In this case the photon flux to the detector is proportional to the solid angle defined by the ratio of the grating area to the square of the monochromator focal length.^{5,6}

A photomultiplier detector was used so that a voltage output proportional to the radiant flux transmitted by the monochromator was produced. The response curve for the type S-13 photo detector used is shown in Fig. 3.⁷ In the figure this response is compared with the S-20 response often used in star tracker navigational systems.⁸ Both types have the greatest sensitivity from approximately 4000 Å to 5000 Å. Unlike the

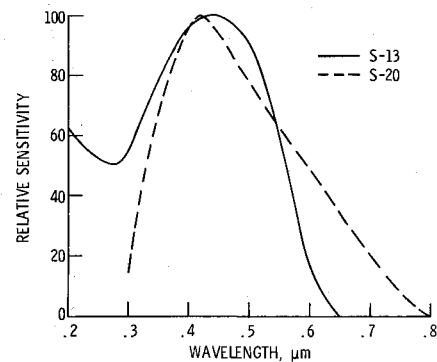


Fig. 3 Phototube spectral response characteristics (Ref. 5).

S-20, however, the S-13 photo detector has a relatively high response to radiation at wavelengths below 3000 Å thus permitting radiance measurements over a wider wavelength range. In the present experiments, the phototube bias was maintained at 1400 v. The magnitude of this voltage determines the amplitude of the measured radiation output, and thus must be the same value for both calibration and thruster data.

The plane grating was designed to provide maximum radiant energy in the first order spectra at 4000 Å, so that instrument sensitivity was greatest at wavelengths of greatest phototube sensitivity. The grating could be rotated to allow analysis of the spectrum between 2800 and 6000 Å. The ruled area of the grating was 27 cm².

System Calibration

The optical system was calibrated using a National Bureau of Standards spectral radiance standard.⁹ This was a tungsten filament lamp operating on a d.c. current of 35 amp. The calibration was performed with the optical arrangement shown in Fig. 2b. The variation in transmissivity with wavelength of the window shown in Fig. 2a was determined by comparing the photo tube signal with and without the window in the optical path. The radiant flux I_λ (w/cm²) incident on the detector can be found from the known spectral radiance $Q(\lambda)$ [w/(cm²)(μ)(sterad)] of the lamp

$$I_\lambda = R(\lambda)Q(\lambda)(\Delta\lambda)\Omega \quad (1)$$

where $R(\lambda)$ accounts for transmission corrections, Ω is the solid angle (sterad) subtended by the monochromator grating at the exit slit, $\Delta\lambda$ is the band width determined by the product of slit width (200 μ) and the monochromator dispersion (16 Å/mm) and was equal to 3.2×10^{-4} μ for all measurements.

Unlike the thruster produced radiation, the strip filament of the calibration lamp did not provide an extended source of light to the monochromator. Hence, a condensing lens was required to provide the illuminance at the monochromator entrance slit needed to fill the grating completely with light. Also, to provide calibration data at the same slit width used in measuring thruster radiances (200 μ), neutral density filters were used to attenuate the incident signals from the lamp. Thus it was necessary to correct for transmission losses through the lens and filter combination in order to use the calibration data to obtain thruster radiances. The transmissivity of the lens was 0.9 over the wavelength range of interest. The variation in transmissivity of the filters with wavelength was less than 2% for a signal reduction by a factor of the order of 10^{-5} .

The radiated power from the lamp dropped off rapidly below 3000 Å, so that the calibrated response was least accurate below this wavelength. This lack of accuracy results from stray light effects, which may account for more than 10% of the detected signal below 3000 Å. Above this wavelength, the stray light contribution was expected to be less than 1%.

The response curve determined in the above manner was used to obtain spectral radiances from measurements of the downstream radiation produced by the thrusters. This was possible

because the amplitude of the signal response at a given wavelength was proportional to the radiant flux transmitted through the monochromator to the photodetector. Because pen deflection on a chart recorder is proportional to the voltage output of the photomultiplier tube, the calibrated detector response is determined in units of w/cm^2 per in. of deflection.

A comparative measurement of the NBS calibrated lamp radiant flux was made using a calibrated thermopile radiometer. Two band pass filters with bandwidths at half-maximum of 100 Å were used with the thermopile radiometer and the NBS lamp as the source. The peak responses of the filters were at 4030 and 5480 Å. A calculation of the integrated radiant flux from the NBS lamp with appropriate filter transmission corrections was compared with the thermopile output using tabulated lamp radiances. The two methods gave radiant flux values that agreed to within 16% at 4030 Å and 29% at 5480 Å.

Other factors that could affect radiance measurements include optical reflectance from tank walls, back flux of propellant reflected or sputtered from tank walls, background tank pressure variations and fluorescence of the quartz window.

Measurements of Optical Reflection from the Tank Wall

Associated with the problem of simulating space radiation effects in a vacuum facility was the possibility of tank wall reflection of thruster discharge chamber light. In the experiment, the section of tank wall intercepted by the optical line of sight was blackened (see Fig. 1). In order to measure the effectiveness of this blackened surface in reducing reflected light into the detector, a 1000-w tungsten-iodide lamp was mounted at thruster location B (Fig. 1) and used to illuminate the tank. An image of the blackened wall area was formed on the monochromator entrance slit.

A reflectance factor $f(\lambda)$ can be defined in terms of the wall reflected lamp signal. From measurements of this factor, it was concluded that the reflected signal from the blackened wall was negligible.

Reflected Propellant Flux from Tank Walls

Thruster beam ions impinge upon the copper cryoliner on the vacuum tank wall, and can be semielastically reflected back toward the thruster as neutral atoms or sputter condensed mercury atoms toward the thruster. The concern here is that such atoms may tend to enhance the neutral atom density in the region of spectral observation, thus introducing an error in radiance measurements. An estimate of this effect can be obtained using the theory developed by Reynolds¹⁰ for the back flux of sputtered atoms in a cylindrical tank and assuming an accommodation coefficient of 0.95 for mercury ions incident on the tank walls.¹¹ From such calculations, it is estimated that the ratio of the back flux density to the neutral efflux density from the thruster is of the order of 0.5%. Thus the effect of back flux density on the mercury atom spectral line amplitudes is negligible.

Effect of Ambient Pressure

The nominal operating pressure of the vacuum facility during the tests was about 10^{-7} torr. Measurements of exhaust plume radiances were also obtained at a tank pressure of about 10^{-5} torr. From such measurements it was concluded that no discernible difference in spectral line amplitudes could be attributed to a change in tank pressure. It should be noted that pressure effects are expected to be negligible below about 10^{-3} torr. Above this pressure atom-atom collision and recombination effects can contribute to atom excitation.

Fluorescence

To determine whether the window used in these experiments fluoresced by absorption of uv radiation, the mercury spectrum was examined in the region of about 4000 Å, where commercial

Table 1 Measured spectral radiances from regions downstream of operating mercury bombardment thrusters

Wavelength, Å	Spectral radiance $N(\lambda)$, w/cm^2 sterad	
	Thruster location A	Thruster location B
2815	7×10^{-10}	8×10^{-11}
2847	$< 2 \times 10^{-11}$	
2967	7×10^{-11}	
3021-3023	1×10^{-10}	
3125-3131	2×10^{-10}	9×10^{-11}
3650-3663	2×10^{-9}	2×10^{-10}
4047	2×10^{-10}	5×10^{-11}
4078	5×10^{-11}	
4347	2×10^{-11}	
4358	4×10^{-10}	9×10^{-11}
4916	2×10^{-11}	
5461	4×10^{-10}	1×10^{-10}

grade fused quartz is known to fluoresce most sharply.¹² If the fluorescent radiation from the window were able to be focused onto the exit slit of the monochromator, a continuum background radiation should have been superimposed on the observed line spectra. The fact that no such continuum was noted to within the sensitivity of the detection system suggests that window fluorescence did not contribute to the line spectrum measurements.

Experimental Results

Separate measurements of the beam spectral radiances were made for thrusters operating at the two locations. The wavelength range investigated was from 2800 Å to 6000 Å. The results are tabulated in Table 1. Spectral radiance values ranged from 10^{-11} to 10^{-9} $\text{w/(cm}^2\text{)(sterad)}$ varying with wavelength. The spectral radiance of the 3650 Å transition was greater than contributions from other transitions by at least a factor of two. The minimum detectable spectral radiance in these experiments was 2×10^{-12} $\text{w/(cm}^2\text{)(sterad)}$. Only those transitions whose radiance exceeded this lower limit in first order are recorded.

Excitation of the mercury ion at 2815 Å was an interesting feature of the investigation. This line was also observed in our earlier spectrographic work. It represents a forbidden transition from the $6s^2 2D_{5/2}$ metastable state of singly ionized mercury. Its existence in the spectrum may be due to direct excitation from the ground state of the atom or ion, or it may represent the last step in a cascade process from higher lying states of ion excitation. In our earlier work² it was argued that the $6s^2 2D_{5/2}$ state is populated from the $6^2P_{3/2}$ level as a result of excitation collisions in the discharge chamber. The resulting metastable ions may then be extracted as beam ions, eventually decaying to the $6^2S_{1/2}$ ion ground state. The calculated lifetime of this metastable state¹³ is of the order of 0.1 sec.

Absolute radiance measurements in the uv below 2800 Å were not within the capability of the optical system used in these tests. It was possible, however, to detect the resonant radiation at 2537 Å in second order. From such measurements it was clear that the radiance of this resonant line exceeded that of the 3650 Å line of Table 1 by one or more orders of magnitude. [In second order, the radiance value of the 2537 Å line was 2×10^{-8} $\text{w/(cm}^2\text{)(sterad)}$.]

Discussion of Results

Source of Observed Radiation

Over the wavelength range of 3000 Å to 6000 Å the dominant light flux is due to excitation of atomic mercury. There was evidence to indicate that the excitation of thruster neutral efflux by beam neutralizing electrons was the dominant process.

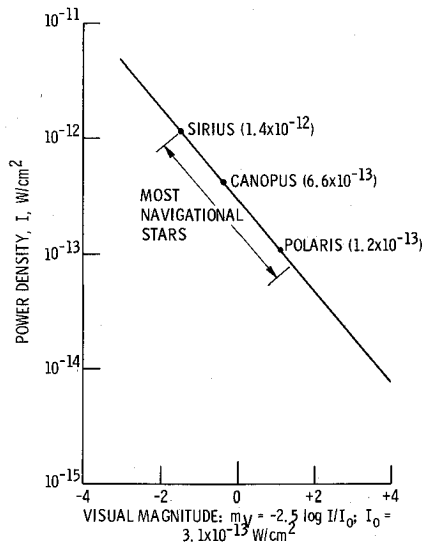


Fig. 4 The relationship between power density and visual magnitude of celestial bodies (Ref. 14).

Radiance levels appeared to be sensitive to large changes in the neutralizer-to-beam coupling voltage, increasing sharply when this voltage rose as a result of lowered neutralizer flow rate. The coupling mechanism determines the effective electron energy and thus the degree of excitation. Further work is required in this area before a full understanding of the processes producing the observed atom excitations can be achieved.

Comparison of Measured Radiances to Navigational Star Signals

The range of radiant power densities in the visible spectral region from navigational stars such as Canopus and Polaris are shown in Fig. 4.¹⁴ Here the total radiant power density in w/cm^2 is plotted as a function of stellar visual magnitude. Navigational star photovisual power densities above the Earth's atmosphere fall in the range 10^{-12} to 10^{-13} w/cm^2 . Polaris, which has a power density of 1.2×10^{-13} w/cm^2 , will be used to compare the magnitude of thruster beam background to star signal. Assuming a star tracker is located relative to a thruster as indicated in Fig. 1, the following analysis may be pursued.

A photoemissive current due to the star light flux without background radiance may be defined as

$$i_s = A \int_{0.3\mu}^{0.8\mu} M(\lambda) \cdot F(\lambda) d\lambda \quad (2)$$

where $A(cm^2)$ is the effective area of the star tracker entrance aperture, $M(\lambda)^{1,15}$ is the star spectral power density in $w/(cm^2)(\mu)$, $F(\lambda)$ in this case is an S-20 phototube radiant sensitivity in amp/w. A photoemission current due just to thruster background light flux is expressed as

$$i_b = A\theta^2 \sum_{\lambda=0.3\mu}^{0.8\mu} N(\lambda)F(\lambda) \quad (3)$$

where θ is the angular width of a field of view of square cross section, $N(\sigma)$ is the measured background radiance [in $w/(cm^2)(sterad)$]. The summation is over the discrete mercury spectrum characteristic of the radiation downstream of a thruster. No attempt was made to evaluate the photosensor signal to noise ratio. Table 1 may serve as background radiance input for evaluation of the signal-to-noise ratio of a particular star tracker configuration. The magnitude of a photosensor output current due to the thruster beam background and the Polaris light flux are considered to be two independent measurements. The relative magnitude of the signals

$$\frac{i_b}{i_s} = \frac{\theta^2 \sum_{\lambda=0.3\mu}^{0.8\mu} N(\lambda) \cdot F(\lambda)}{\int_{0.3\mu}^{0.8\mu} M(\lambda) \cdot F(\lambda) d\lambda}$$

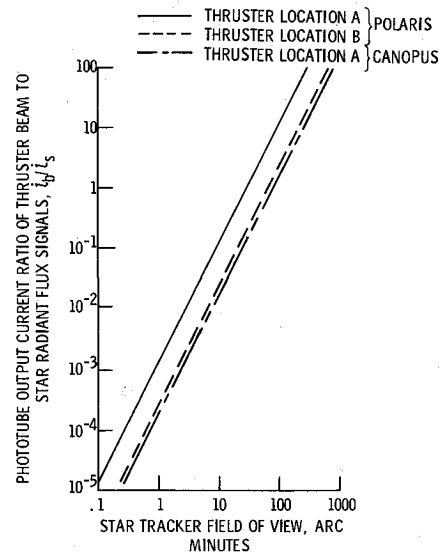


Fig. 5 Phototube output current ratio of thruster beam to star radiant flux signals. Assume square star tracker field aperture. S-20 phototube response. Wavelength range $0.3-0.8 \mu$.

is shown in Fig. 5. For thruster locations A and B (Fig. 1), the background and Polaris signals are equal for fields of view of 28 and 65 arc min, respectively.

Star trackers generally use modulation of the light flux at the field aperture and may also incorporate an image dissector at this aperture to reduce background effects.¹⁶ Using such a modulated system, an instantaneous field of view of 10 arc min would yield a background to Polaris signal ratio of 0.1 for thruster location A. Using this modulation process with an image dissector, an instantaneous field of view as low as 1 arc min may be obtained. For an instantaneous field of view of 1 arc min, the ratio of thruster background radiant flux to Polaris radiant flux signals would be of the order 0.001 for thruster location A. Results shown in Fig. 5 further indicate that the thruster exhaust beam interference is reduced by approximately a factor of 8 when Canopus is the navigational reference.

The preceding analysis is based on the assumption that a star tracker would be required to view through the thruster exhaust as shown in Fig. 1. The results of Fig. 5 indicate viewing the thruster exhaust in a region of lower neutral density (e.g., thruster position B) decreases the background effect by a factor of 5. A star tracker viewing outside the 2π solid angle defined by the beam exhaust direction (Fig. 1) should encounter essentially no thruster background interference.

It should be noted that although mercury resonant radiation may have intensities several orders of magnitude greater than the strong 3650 Å transition, the wavelengths corresponding to this type of radiation are in the ultraviolet and would be outside the normal tracker sensitivity.

Extrapolation of Results to uv and ir

Although the ultraviolet and infrared regions of the spectrum lie outside the range of sensitivity of star tracker systems, other devices on board a spacecraft, such as spectrometers and radiative temperature sensors, could be affected by contaminant radiation of the type described herein. The strong resonant line at 2537 Å previously mentioned as having been observed implies the existence of other strong resonant radiation at 1650, 1850, and 1942 Å. In addition, other ultraviolet lines were observed in second order (e.g., at 2815 and 2262 Å). There are known strong mercury lines in the infrared at 10,140 and 11,287 Å.¹⁷ All such lines may present a potential source of interference to various types of scientific experiments on a spacecraft.

Guidelines to Reduce Interference with Optical Sensors

As a result of the information generated in the present investigation, the following guidelines should be considered relative to thruster radiative interference with optical systems. a) If possible, locate view axes of the optical systems on board a spacecraft so as not to view downstream of operating thrusters. All data in the present study were obtained viewing through the thruster beam exhaust. Data indicate that thruster beam radiance substantially decreases as the viewing angle of the optical sensor is directed toward regions of lower mercury neutral density. b) If the star tracker viewing angle must intersect the thruster exhaust, thruster background interference may be reduced by operating the optical system with a sufficiently small field of view along with light baffles to reduce reflection. For example, the Polaris signal from an optical system viewing through the exhaust one meter downstream of the thruster would be approximately 1000 times greater than the thruster background effect. In this case the optical system would employ light flux modulation, image dissection, and an instantaneous field of view of 1 arc min. c) During spacecraft acquisition for which a star tracker field of view of a few degrees may be employed, a poorly chosen sensor view angle could yield deleterious results. Here, of course, it is assumed that mission requirements would dictate that a 30-cm-diam thruster be operational during the spacecraft acquisition. d) Improvements in thruster technology may reduce downstream atom densities and neutralizing electron coupling energy. Both parameters are directly related to the radiation produced in the thruster beam. At present, there is insufficient data available to understand fully all the ramifications of such technological improvements on the level of downstream radiation. To gain such understanding, more work is required in determining the source of the observed radiation. e) For some missions it is possible to substitute a sun sensor¹⁸ for spacecraft control functions. In such cases the problem of thruster-produced radiation would have to be investigated as a possible source of sensor interference. Because the solar radiant power density is much larger than stellar radiant power densities, the interference problem should be much less for sun sensors than for star trackers.

A more complete appraisal of the problem of optical radiation interference described herein will require experiments with prototype systems. In such experiments the geometrical relationship between the thruster and optical instrumentation for a given spacecraft would be investigated.

Concluding Remarks

A 0.5-m focal length, plane grating monochromator was used to measure the radiance of spectral radiation emanating from regions downstream of a mercury bombardment thruster. The wavelength range investigated was 2800 Å to 6000 Å. This radiation was due primarily to the radiative decay of excited mercury atoms exhausted from the thruster. Radiance values ranged from 10^{-11} to 10^{-9} W/(cm²)(sterad), varying with wavelength. For resonant radiation, the spectral radiance exceeds 10^{-8} W/(cm²)(sterad). These values are accurate to within 29% based on thermopile radiometer measurement of the calibration source. Extrapolating the results to the ultraviolet as well as the infrared suggests that thruster produced radiation could also

interfere with uv and ir sensitive experiments on board a spacecraft.

From such radiance measurements, it was concluded that thruster background radiation should not interfere with the control functions of a star tracker viewing through the thruster exhaust, provided that the tracker is designed to operate with a sufficiently small field of view. Problems may be encountered, however, during the spacecraft acquisition phase where a larger field of view may be required. Here the thruster exhaust radiation may be comparable to the star light flux. This problem may be circumvented by locating the tracker view axis so as not to view downstream of an operating thruster. The thruster radiative interference should be negligible in this case due to the low concentration of neutral mercury in the tracker field of view.

References

- ¹ "A Study of the Effects of a Cesium Ion Thruster Upon a Polaris Star Tracker," Rept., HIT-452, May 1970, Hittman Associates Inc., Columbia, Md.
- ² Milder, N. L., "Potential Star Tracker Interference from Radiation Produced by Mercury Bombardment Thrusters," TM X-67858, 1971, NASA.
- ³ Rawlin, V. K., Banks, B. A., and Byers, D. C., "Design, Fabrication, and Operation of Dished Accelerator Grids on a 30-cm Ion Thruster," AIAA Paper 72-486, New York, 1972.
- ⁴ Bechtel, R. T., "Performance of a Neutralizer for Electron Bombardment Thruster," AIAA Paper 72-207, New York, 1972.
- ⁵ Sawyer, R. A., *Experimental Spectroscopy*, Dover Publications, New York, 1963, Chap. 3.
- ⁶ Turner, E. B., "Optical and Ultraviolet Techniques," *Plasma Diagnostic Techniques*, edited by R. H. Huddleston and S. L. Leonard, Academic Press, New York, 1965, pp. 319-358.
- ⁷ RCA *Electron Tube Handbook*, HB-3, Radio Corporation of America, Harrison, N.J., 1967.
- ⁸ "Spacecraft Star Trackers," NASA SP-8026, 1970.
- ⁹ Stair, R., Johnston, R. G., and Halbach, E. W., "Standard of Spectral Radiance for the Region of 0.25 to 2.6 Microns," *Journal of Research of the National Bureau of Standards-A, Physics and Chemistry*, Vol. 64A, No. 4, July-Aug. 1960, pp. 291-296.
- ¹⁰ Reynolds, T. W., "Mathematical Representation of Current Density Profiles from Ion Thrusters," TN D-6334, 1971, NASA.
- ¹¹ Childs, J. H., "Design of Ion Rockets and Test Facilities," IAS Paper 59-103, New York, 1950.
- ¹² "Optical Fused Quartz and Fused Silica," Pamphlet EM-9227, 1970, Amersil Inc., Hillside, N.J.
- ¹³ Garstang, R. H., "Transition Probabilities of Forbidden Lines," *Journal of the National Bureau of Standards-A, Physics and Chemistry*, Vol. 68, No. 1, Jan.-Feb. 1964, pp. 61-73.
- ¹⁴ Abate, J. E., "Star Tracking and Scanning Systems: Their Performance and Parametric Design," *Transactions of the IEEE, Aerospace and Navigational Electronics*, Vol. ANE-10, No. 3, Sept. 1963, pp. 171-181.
- ¹⁵ Naqvi, A. M. and Levy, R. J., "Some Astronomical and Geophysical Considerations for Space Navigation," *Transactions of the IEEE, Aerospace and Navigational Electronics*, Vol. ANE-10, No. 3, Sept. 1963, pp. 154-170.
- ¹⁶ McCannless, F. V., "A Systems Approach to Star Trackers," *Transactions of the IEEE, Aerospace and Navigational Electronics*, Vol. ANE-10, No. 3, Sept. 1963, pp. 182-193.
- ¹⁷ Anderson, R. J., Lee, E. T. P., and Lin, C. C., "Electron Excitation Functions of Mercury," *Physical Review*, Vol. 157, No. 1, May 5, 1967, pp. 31-40.
- ¹⁸ "Spacecraft Sun Sensors," NASA SP-8047, 1971.